IEEE Journal of Microwaves

Received 10 June 2021; revised 13 August 2021, 9 September 2021, and 16 September 2021; accepted 17 September 2021. Date of publication 27 October 2021; date of current version 7 January 2022.

Digital Object Identifier 10.1109/JMW.2021.3115244

Bandwidth and Center Frequency Reconfigurable Waveguide Filter Based on Liquid Crystal Technology

FYNN KAMRATH [1], ERSIN POLAT [2], STIPO MATIC [2], CHRISTIAN SCHUSTER [2], DANIEL MIEK [1] (Student Member, IEEE), HENNING TESMER [2], PATRICK BOE [1] (Student Member, IEEE), DONGWEI WANG [2], ROLF JAKOBY [2] (Member, IEEE), HOLGER MAUNE [3] (Senior Member, IEEE), AND MICHAEL HÖFT [1] (Senior Member, IEEE)

(Regular Paper)

[1]Chair of Microwave Engineering, Kiel University, 24143 Kiel, Germany
[2]Institute for Microwave Engineering and Photonics, Technische Universität Darmstadt, 64289 Darmstadt, Germany
[3]Chair of Microwave and Communication Engineering, Otto von Guericke University, 39106 Magdeburg, Germany

CORRESPONDING AUTHORS: Fynn Kamrath; Ersin Polat (e-mail: flk@tf.uni-kiel.de; ersin.polat@tu-darmstadt.de).

This work was supported by the Deutsche Forschungsgemeinschaft (DFG, German Research Foundation)-424862129 and the DFG funding program Open Access Publizieren.
(Fynn Kamrath and Ersin Polat are co-first authors.)

ABSTRACT This paper presents for the first time a fully electronically reconfigurable waveguide filter tunable in bandwidth and center frequency based on liquid crystal (LC) technology. A continuously reconfigurable two pole bandpass filter is designed and characterized in the Ka-band at 30 GHz. To be able to tune both center frequency and bandwidth independently, the resonators and coupling structures are filled with LC as tunable material. Hence, the filter's center frequency and coupling strengths can be tuned and, furthermore, tuning with constant filter characteristic is possible. To tune the LC, a novel two-layer electrode design for waveguide structures is presented, which is simple to integrate and provides a high tuning efficiency with low insertion loss. By applying different bias configurations, the LC's effective permittivity can be varied, and therefore, also the resonators' electrical lengths. The presented two pole filter can adapt its center frequency from 29.8 GHz to 30.7 GHz with a maximum 3 dB bandwidth variation from 660 MHz to 870 MHz. The measurements are carried out with bias voltages up to ±250 V.

INDEX TERMS Microwave filter, liquid crystals, millimeter wave communication, tunable circuits and devices, K-band.

I. INTRODUCTION

Wireless communication systems, such as mobile or satellite communication, must provide ever higher data rates and new services for a rapidly growing number of users. This constant challenge is complicated by the limited frequency spectrum [1]–[4]. Therefore, new technologies have been developed to use the spectrum as efficiently as possible, e.g. improved modulation techniques [5]. Moreover, the millimeter wave (mmWave) frequency bands are gaining more interest for communication systems, since larger absolute bandwidths are available [6], [7]. A further opportunity is to apply reconfigurable RF front-ends, especially for bandless concepts like software defined radio or cognitive radio. A key component for such reconfigurable RF front-end devices are tunable filters [8], [9]. State-of-the-art RF front-ends consist of filter banks with a multitude of bandpass filters, which cover a plurality of parameters such as center frequency and bandwidth. The design is based on a fixed number of control states that can only be set discretely and do not allow subsequent reconfiguration of filters or frequency band allocations. Furthermore, the large volume and weight of filter banks is a major problem especially for satellites. By using tunable filters, parameters such as center frequency and bandwidth can be adjusted continuously within a certain tuning range. This

allows an almost unlimited number of configurations of the RF front-end. Hence, the spectrum efficiency can be increased by multiband operation, frequency hopping and, furthermore, the system can be adapted to new services and standards [10].

In general, reconfigurable filters refer to either adjustable center frequency, bandwidth, or both. In the literature, different tuning mechanisms are used for realizing reconfigurable filters, e.g.: semiconductors [11], [12], microelectromechanical systems (MEMS) [13], [14], barium strontium titanate (BST) [15]–[17] and liquid crystals (LC) [18]–[20]. Coaxial, dielectric and waveguide filters are mostly tuned by mechanical means, e.g. a tuning screw [21], [22]. All mechanical tuning mechanisms require good electrical contact, which can be difficult to achieve. A severe degradation of the Q-factor can be the result of a non-optimal connection. In this aspect, electrical tuning mechanism are superior since no moving parts are required. For the Ka-band, semiconductors and BST have comparatively high losses, hence MEMS are mostly used for tunable filters in this frequency band.

In this work, LC technology is applied as an alternative technology, since it has relatively low loss in the mmWave regime even up to several THz [23], [24], high linearity [25] and is continuously tunable. It has also been investigated for tunable filters for space applications, for which LC has excellent properties, e.g. its power consumption for tuning is very low, because only quasi-static electric fields are necessary, it has no mechanical moving parts which can cause wear-out failures and it is qualified for the harsh space environment [26]. Furthermore, a first tunable LC filter demonstrator will be tested in space in the Heinrich Hertz mission [27], which will be launched in 2022. However, to the best of the authors' knowledge electronically reconfigurable bandpass filters in the mmWave regime reported so far are only tunable in either center frequency or bandwidth. For a fully reconfigurable RF front-end the filters must be independently tunable in both. In previous work [20], a center frequency tunable LC filter with non-tunable coupling elements has been reported at 60 GHz. To obtain tunability in both center frequency and bandwidth, LC tunable resonators and coupling elements are used in this work. In [28] a bandwidth and center frequency tunable bandstop filter in half-mode substrate integrated waveguide (HMSIW) technology has been developed. However, the tuning is achieved by detuning resonators and not by adjusting the required coupling, resulting in a distorted performance.

II. MICROWAVE LIQUID CRYSTAL TECHNOLOGY

In the past two decades, research of LCs for microwave applications has been established, resulting in various devices e.g. steerable antenna arrays [29], tunable filters [20], switches [30], phase shifters [31] and power dividers [32]. A detailed summary of LC applications in the mmWave regime is given in [33]. Thermotropic LCs have different mesophases between a solid crystal and an isotropic liquid. In this work, calamatic LCs are used in their nematic phase, where they are liquid and at the same time they have properties of a crystal. Hence, they can flow like a liquid and the rod-like shaped molecules have simultaneously an orientational order. That is why nematic LCs show anisotropy and birefringence. The long and short axis of the molecules have the relative permittivities $\varepsilon_{r,\parallel}$ and $\varepsilon_{r,\perp}$, respectively, resulting in an anisotropy defined by $\Delta\varepsilon = \varepsilon_{r,\parallel} - \varepsilon_{r,\perp}$ [34]. A further property of LCs is that the molecules tend to align themselves parallel along their long axis. Hence, the mean direction of the molecules inside a unit volume element can be described macroscopically by the unit vector $\vec{n}$, the so-called director. Depending on the orientation of the director $\vec{n}$ to the applied RF field, the LC's permittivity can continuously be changed between two extreme states, which are for parallel and orthogonal orientation resulting in a permittivity of $\varepsilon_{r,\parallel}$ and $\varepsilon_{r,\perp}$, respectively. For tuning, an external bias field is necessary, either a quasi-static electrical or magnetic field, since the molecules are aligning themselves parallel to the bias field lines. A very detailed summary of microwave LC technology is given in [35]. In this work, the LC mixture licriOn^{TM} GT7-29001 from Merck KGaA is used, which is specifically optimized and synthesized for microwave applications. Its permittivity ranges from $\varepsilon_{r,\parallel} = 3.53$ to $\varepsilon_{r,\perp} = 2.46$ with a dissipation factor between $\tan\delta_{\parallel} = 0.0064$ and $\tan\delta_{\perp} = 0.0116$ at 19 GHz [36].

III. RECONFIGURABLE FILTER THEORY

The applied tuning mechanism for waveguide filters was first reported in [37], however with mechanical moving parts. In this work, LC is used as tuning technology and, therefore, the filter is electronically reconfigurable. Reconfigurable impedance inverters are introduced, which can be used to adjust the coupling strength between two resonators. These reconfigurable impedance inverters are realized as non resonating resonators and are called coupling resonators (CR) while the conventional resonators, which form the passband, are called main resonators (MR). By changing the resonance frequency of the CR, the inverter value K can be adjusted which influences the inter-resonator coupling. This can be seen from:

$$\frac{K_{0,1}}{Z_0} = \frac{K_{n,n+1}}{Z_0} = \sqrt{\frac{\pi\Delta}{2g_0g_1}}, \quad \text{and,} \tag{1}$$

$$\frac{K_{i,j}}{Z_0} = \frac{\pi\Delta}{2\sqrt{g_i g_j}}, \qquad i = 1, 2, \ldots, n-1; \quad j = i+1, \tag{2}$$

with $\Delta = \frac{\lambda_{g1}-\lambda_{g2}}{\lambda_{g0}}$. The guide wavelengths at the band-edge frequencies are denoted as λ_{g1} and λ_{g2}, while λ_{g0} is the guide wavelength at the center frequency [38]. The g values represent the lumped-element lowpass prototype elements and are calculated from filter properties like return loss RL and filter order n. These properties are design parameters which do not change, which means that the g values remain constant. Therefore, a change of the inverter value K causes a shift in the band-edge frequencies. For a proper bandwidth (BW) change, both, the inter-resonator coupling as well as the input/output

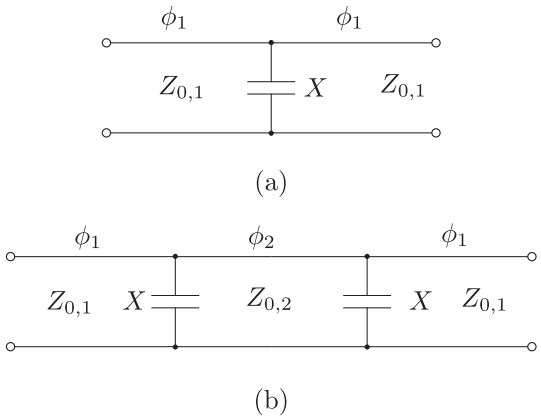

FIGURE 1. Impedance inverter model with (a) transmission lines ϕ_1 and reactance X and (b) inverter model with coupling resonator.

coupling need to be changed to support the different bandwidths. The square root in (1) causes different scalings of the inverter values, which means that different tuning ranges of input/output and inter-resonator coupling are required.

In Fig. 1, two different equivalent circuits for inverter models are shown. Fig. 1(a) shows the classical inverter model, where the characteristic impedances $Z_0 = Z_{0,1}$ on both sides are identical [38]. The line length ϕ_1 represents the loading effect on the adjacent resonators. If the reactance X is negative, the line lengths are positive and if the reactance is positive, the line lengths are negative. This line length influences the electrical length of the connected resonators and causes a shift in resonance frequency. For identical Z_0 both line lengths ϕ_1 are identical as well. For example, in waveguide technology an inverter is often realized as an inductive iris aperture which influences the adjacent resonators. In Fig. 1(b) the model is extended to include a coupling resonator [39]. In this case ϕ_2 represents the electrical length of the coupling resonator and its characteristic impedance $Z_{0,2}$. In waveguide technology the structure consists of a coupling resonator embedded between two iris apertures. It can be seen that both iris apertures are identical and, therefore, only the electrical length of the resonator ϕ_2 needs to be varied to realize different inverter values.

By alternating CRs and MRs it is possible to create a fully reconfigurable filter, since each coupling can be adjusted individually. By utilizing this technique the problem of changing the coupling is shifted to changing the resonance frequency of resonators. In [37] this working principle is used to create a fourth order bandpass filter with one cross coupling with a variable center frequency and bandwidth. Furthermore, coupling resonators are able to introduce a coupling sign change by adjusting its resonance frequency [40].

While coupling resonators allow for a continuous bandwidth change, they come with disadvantages as well. These filter structures require at least $n + 1$ additional resonators resonating below or above the passband to achieve full reconfigurability, which can affect performance in the stopband.

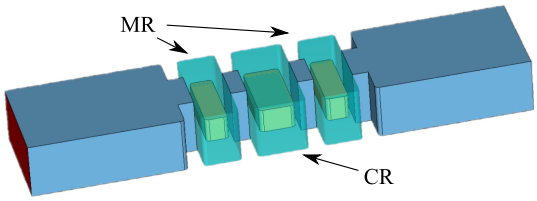

FIGURE 2. 3D-model for coupling factor study with two main resonators (MR) and one coupling resonator (CR).

IV. FILTER DESIGN

This work aims to develop a center frequency and bandwidth tunable bandpass filter based on LC technology in the Ka-band. A center frequency of 30 GHz with an intermediate equal ripple bandwidth of 300 MHz is chosen as a starting point for the filter design. The bandpass filter consists of five resonators in total, which means two resonators will form the passband, while three coupling resonators are used to enable the bandwidth tuning.

To prevent the LC from leaking, it is necessary to encase it in Rexolite cavities. To create a robust enclosure, a minimum wall thickness of 0.5 mm is chosen. A high tuning range of the coupling resonators results in a high bandwidth change in the passband. Therefore, the coupling resonators are dimensioned to operate below the Ka-band to increase the volume filled with LC. This results in a completely spurious free Ka-band, while the coupling resonators are comparatively large and are filled with more LC. This approach results in a good stopband performance and offers a large tuning range.

As previously mentioned, the resonance frequency of the coupling resonator influences the inter-resonator coupling, and therefore, the bandwidth of the filter. The frequency range of the Ka-band ranges from 26.5 GHz to 40 GHz. This means that the coupling resonators should have a maximum resonance frequency of 26 GHz to prevent spurious resonances in the operating band. The CR resonance frequency at an intermediate tuning state (e.g. $\varepsilon_{r,LC} = 3$) has a direct influence on the bandwidth tuning range of the filter. In general, the closer the CR resonance frequency is to the passband, the stronger is the coupling. To demonstrate this behavior a CST model consisting of two main resonators and one coupling resonator, to tune the inter-resonator coupling, is created. The model is shown in Fig. 2. The coupling resonator is dimensioned such that the resonance frequency is at 24 GHz, 25 GHz and 26 GHz, respectively. The S-parameters can be seen in Fig. 3. Then the permittivity of the CR is varied and the coupling factor M_{12} is extracted through coupling matrix extraction [41]. For the extraction $f_1 = 29.85$ GHz, $f_2 = 30.15$ GHz and RL$= 20$ dB is assumed. The different coupling factors are shown in Fig. 4. The values are normalized to $\varepsilon_{LC12} = 3$ so that only the difference is displayed, which causes all three graphs to pass through $\Delta\ M_{12} = 0$. It can be seen that a higher tuning range can be achieved if the coupling resonator is dimensioned that the resonance frequency is closer to the passband.

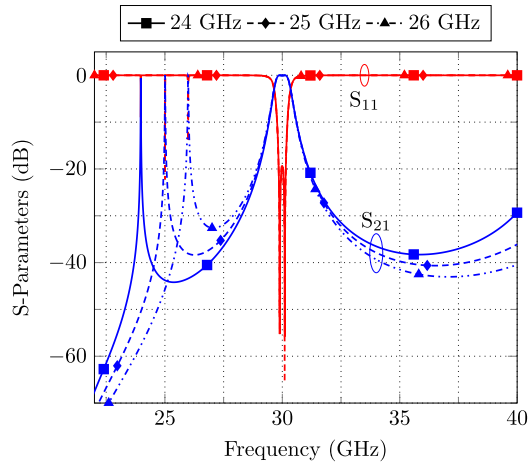

FIGURE 3. Simulated S-Parameters of different coupling resonator resonance frequencies of the structure in Fig. 2. Filter dimensions have been slightly adjusted to achieve 300 MHz BW at $f_0 = 30$ GHz. Permittivity of all LC cavities is assumed to be $\varepsilon_{r,LC} = 3$.

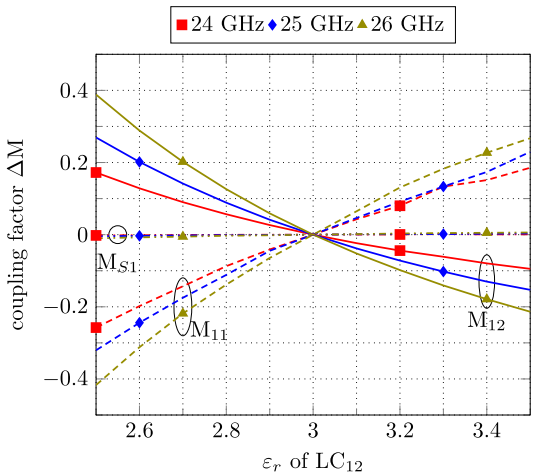

FIGURE 4. Influence of the coupling resonator resonance with respect to its inter-resonator coupling tuning range of the structure in Fig. 2. A larger variance in M_{12} can be observed for resonance frequencies closer to the passband. The permittivity of other resonators is unchanged and remains at $\varepsilon_r = 3$.

Furthermore, the influence on the other coupling factors is displayed. No significant influence on the input/output coupling is recorded while a small influence on the main resonators can be noticed. Since the main resonators are tunable as well, this influence can be compensated. Therefore, it is desirable to dimension the coupling resonator in a way that a high tuning range is achieved, while the spurious resonance does not enter the Ka-band. One additional resonator is added to the input and output, respectively, to create an adjustable external coupling. The symmetric filter model including its dimensions is shown in Fig. 5. The input and output coupling require a smaller tuning range in comparison to the inter-resonator coupling (compare (1),(2)), which allows for an even lower placement of the resonance frequency. Since all cavities are filled with Rexolite and LC,

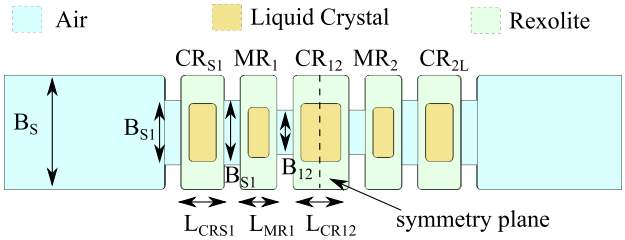

FIGURE 5. Fully reconfigurable filter model. Dimensions in mm: $L_{CRS1} = 2.7$, $L_{MR1} = 2.3$, $L_{CR12} = 3.5$, $B_S = 7.112$, $B_{S1} = 4$, $B_{12} = 2.77$. The filter is symmetric with respect to the resonator CR_{12}. The height of the structure is 3.556 mm, in accordance with the WR-28 standard.

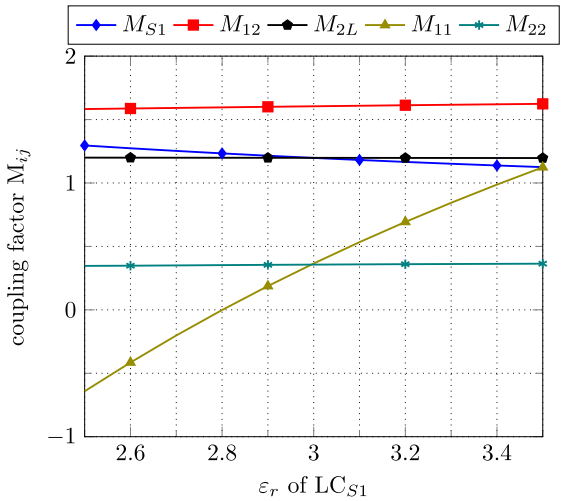

FIGURE 6. Influence of the coupling resonator CR_{S1} towards the other coupling coefficients. Other inter-resonator couplings are mostly unaffected, while an influence on M_{11} can be noted. The permittivity of the other resonators is unchanged and remains at $\varepsilon_r = 3$.

the wavelengths are shortened significantly, which causes all resonator lengths to be between 2.3 mm and 3.5 mm. The widths of the LC cavities are 3.11 mm for the main resonators and 3.61 mm for the coupling resonators, respectively. All LC cavities have a height of 1.56 mm.

In Fig. 6 the influence of the CR_{S1} is shown towards each other coupling factor of the two pole filter. As can be seen, only the input coupling and the main resonator are significantly influenced while the other couplings maintain their values. The inter-resonator coupling is not influenced by the CR_{S1} which means that an independent design of CR_{12} is possible. The coupling factors from the previous analysis can be converted to bandwidth values using (3) and (4) to analyze which bandwidths are supported by this filter structure.

$$M_{12} = k_{12} \cdot FBW^{-1} \tag{3}$$

$$Q_e = \frac{1}{(M_{S1})^2 \cdot FBW} \tag{4}$$

with $FBW = \frac{f_2 - f_1}{f_0}$ [42]. The inter-resonator coupling M_{12} is the coupling matrix value for the lowpass prototype and is equal to $M_{12} = 1.65$ for a second order filter with a return

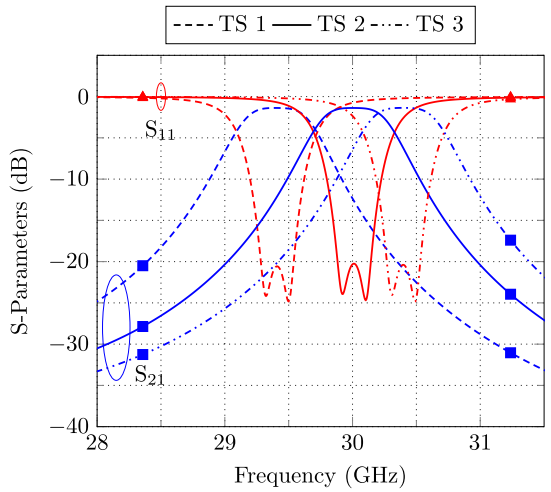

FIGURE 7. Simulated 270 MHz equal ripple bandwidth tuning states (TS) at different center frequencies ranging from 29.41 GHz to 30.41 GHz.

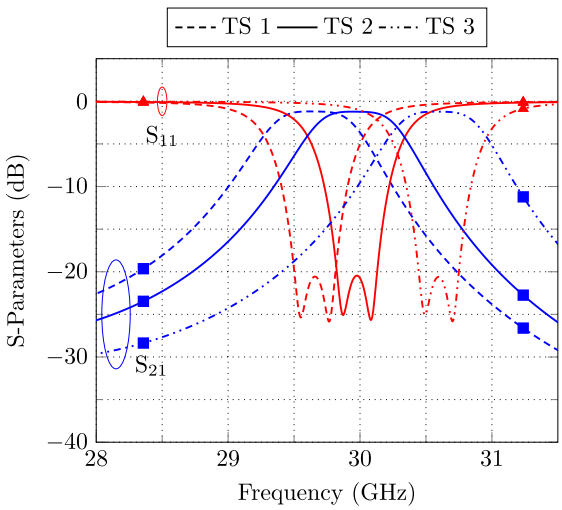

FIGURE 8. Simulated 320 MHz equal ripple bandwidth tuning states (TS) at different center frequencies ranging from 29.66 GHz to 30.60 GHz.

loss of RL = 20 dB. By changing the resonance frequency of CR_{12}, the coupling coefficient k_{12} changes as well. Since the value of M_{12} is fixed this causes a change in the bandwidth. The inter-resonator coupling allows for a equal ripple bandwidth change between 276 MHz and 335 MHz and the input/output coupling supports a equal ripple bandwidth change from 270 MHz to 355 MHz for a center frequency of $f_0 = 30$ GHz. This results in a 3-dB bandwidth tuning range from 640 MHz to 760 MHz. In this case, the inter-resonator coupling is the limiting factor for the simulated tuning range. If small distortions are acceptable, the tuning range can be extended further.

Rexolite is chosen as LC casing, since its dielectric permittivity of $\varepsilon_r = 2.53$ is in the range of the used LC mixture, it has very low losses given by $\tan\delta = 0.66 \cdot 10^{-3}$ and it is space-approved. Brass is used for the waveguide structure. In Fig. 7 and Fig. 8 different tuning states can be seen. This includes a tuning state at 30 GHz and the minimum/maximum frequency where a return loss of 20 dB can be reached. Small interactions between the main and coupling resonators result in a reduction of the maximum achievable bandwidth. Furthermore, since the CRs have an influence on the MRs, a small frequency shift can be seen.

V. ELECTRODE DESIGN

To electrically tune the direction of the LC molecules and, thus, its permittivity, an external quasi-static electric bias field has to be applied inside the resonators. Therefore, an electrode system has to be integrated into the waveguide, which must enable an independent tuning of each resonator individually. To obtain a high tuning efficiency, homogeneous bias field lines are necessary for each tuning state, which is complicated by the waveguide's metal walls, since they are deforming the field lines. Hence, the electrodes must be designed in such a way that the bias fields are as homogeneous as possible.

To orientate the LC parallel to the TE_{101} mode, an electrode, which has at least the width of the LC cavity, is placed on the top and bottom wall of the waveguide, see Fig. 9(a). By applying a voltage that is above a certain threshold voltage [35], the molecules align themselves parallel to the bias field lines and thus parallel to the RF field. In the simulation, a bias of ±250 V is applied, resulting in a very homogeneous bias field, as shown in the results in Fig. 9(a). For orthogonal orientation, two more electrodes are necessary on the waveguide's top and bottom wall. By applying a bias configuration as depicted in 9 d, a quadruple field is generated, which is almost orthogonal to the RF field inside the LC cavity. This results in a less homogeneous bias field, especially in the corners of the LC cavity, leading to a lower tuning efficiency. For filter tuning, the LC molecules' direction and consequentially the permittivity must be continuously tunable between the two extreme states. This is achieved by applying both bias configurations, see Fig. 9(b) and 9(c).

The main challenge for LC waveguide components is the integration of the electrodes [18], [23]. To apply bias to the electrodes, bias lines have to lead in through slots into the waveguide. Furthermore, isolation between bias lines and waveguide must be ensured and the waveguide must be properly sealed to avoid RF leakage. State-of-the-art LC components consist of electrodes which are processed on single layer substrate [20], [43], [44]. They have to be precisely cut, aligned and glued into the waveguide, which causes additional losses. Moreover, misalignment or inaccurate gluing reduce yield. Hence, a novel electrode concept for waveguide LC components is developed, as presented in Fig. 10. It consists of two substrate layers, with the electrode structures in between, as shown in Fig. 10(a). Therefore, isolation is guaranteed. Furthermore, no gluing is needed, since the bottom layer is made out of copper the electrodes can be fixed by pressure. By using alignment pins, misalignment of the electrodes is prevented. To avoid RF leakage, a via fence from the top to the bottom layer is designed, see Fig. 10(b) and 10(c). As shown in Fig. 10(b), the center electrode has a stepped-impedance

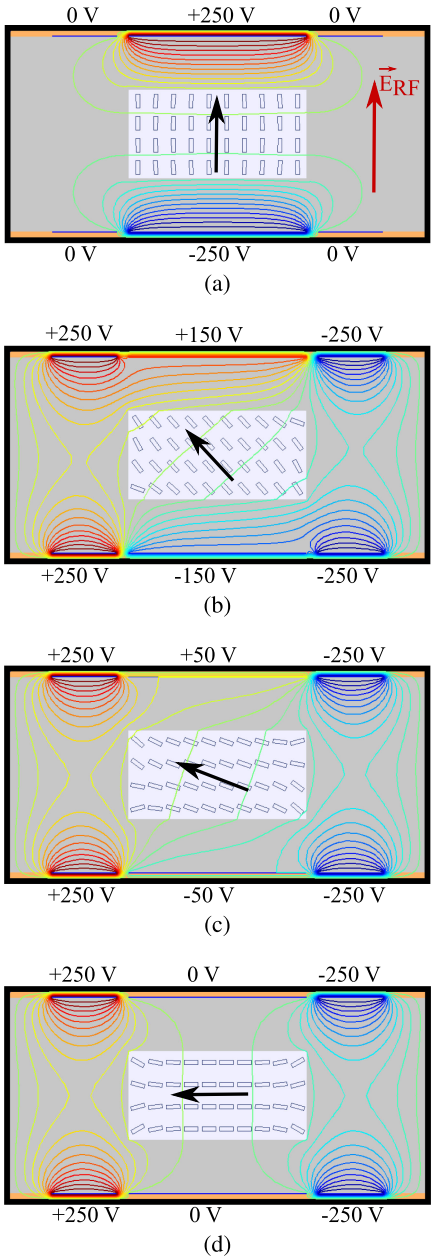

FIGURE 9. LC director dynamic simulation results of an LC waveguide resonator for different bias configurations. Three electrodes are placed on the resonator's top and bottom wall, respectively. The red arrow in 9(a) presents the polarization of the RF field, whereas the black arrows indicates the mean direction of the LC molecules. 9(a) and 9(d) show the results for parallel and orthogonal orientation, respectively. In 9(b) and 9(c) two intermediate states are depicted.

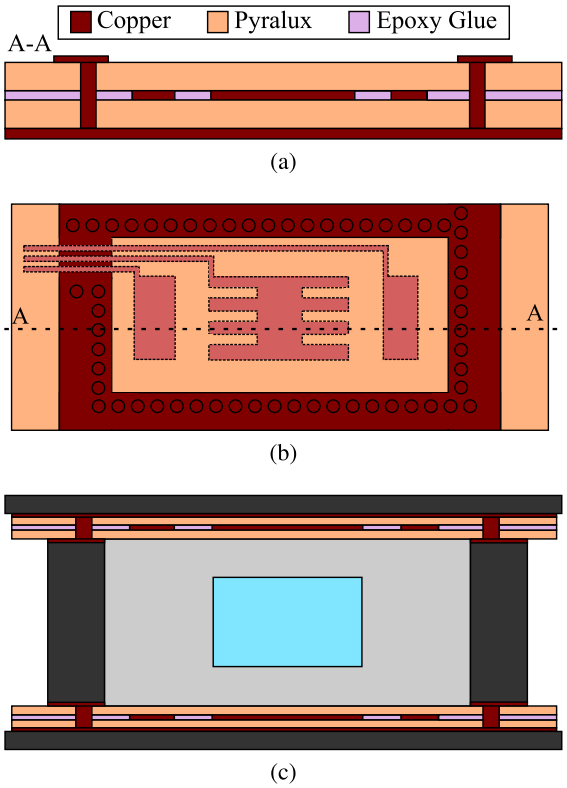

FIGURE 10. In 10(a), a drawing of the cross section of the double layer electrode design is presented. 10(b) shows the top view. and 10(c) the integration of the electrodes into the waveguide.

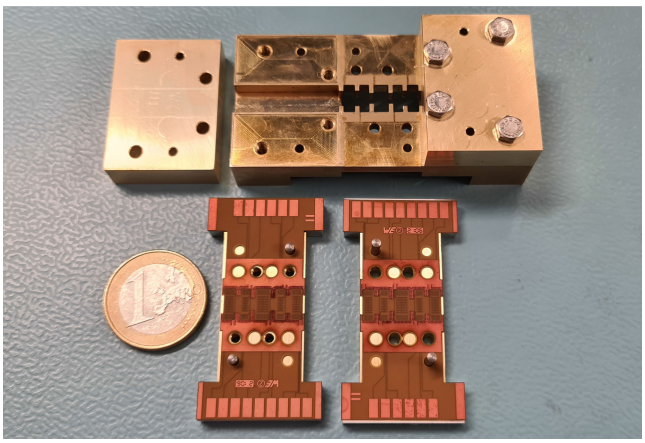

FIGURE 11. Photograph of the fabricated and partly assembled filter. The electrode are placed on two brass plates, which will be screwed on above and below the resonators, after the LC filled Rexolite cavities are inserted.

structure to avoid parasitic mode excitation in the Pyralux substrate, which is explained in detail in [43].

VI. FABRICATION AND CHARACTERIZATION

To integrate the electrodes into the filter, the waveguide filter structure is manufactured in five parts out of brass. It consists of a middle part, in which the resonators are milled, and a bottom and top plate, on which the electrodes are placed by using alignment pins, as shown in Fig. 11. The electrodes are manufactured by Würth Elektronik GmbH & Co KG using 25μm thin DuPont Pyralux AP laminate with a dielectric constant of $\varepsilon_r = 3.4$ and a loss tangent of $\tan\delta = 0.5 \cdot 10^{-2}$. The Rexolite casings are fabricated in two halves with tongue and groove, which are glued together with an UV adhesive, see Fig. 12. The LC is injected into the cavities through a filling hole and is sealed by using an epoxy adhesive afterwards. Finally, the cavities are inserted into the waveguide, which is closed by

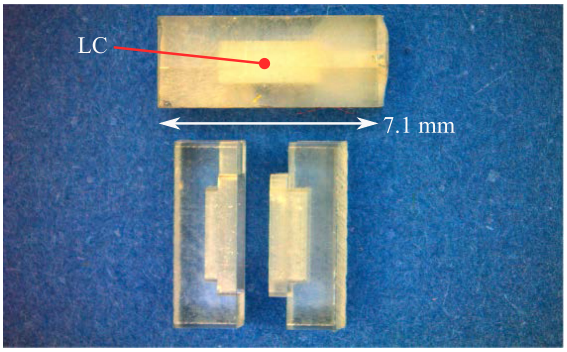

FIGURE 12. **In the bottom, two fabricated Rexolite parts are shown, which are milled with tongue and groove. On the top a LC filled and sealed Rexolite cavity is shown.**

screws on the top and bottom plates. For characterization a Keysight PNA-X network analyzer and a 12 channel voltage source providing a 1 kHz rectangular bias up to ±250 V are used, with a low power consumption of maximum 1.2 W.

In Fig. 13 a, two tuning states for a high center frequency of $f_0 = 30.65$ GHz are shown. The 3-dB bandwidth change from 654 MHz to 827 MHz is clearly visible, while the center frequency is maintained. A small deviation can be noticed as a result of manual adjustment of the bias voltages. In Fig. 13(b) the low center frequency tuning states can be seen. A small frequency shift between the two tuning states can be observed as a result of the influence of the CR on the main resonators. The measured insertion loss (IL) is in the range of 3.5 to 4.2 dB and is higher than the simulation results shown in Section IV. In the simplified simulation model, however, the electrodes and adhesives were not considered because the thin layers and the structure increase the computational effort enormously. Therefore, the simulation was conducted only for the lossiest case of liquid crystal. To analyze the insertion loss, the simulation model has been optimized by including the electrodes and adhesives. The results are summarized in Fig. 14. Since the adhesives are not characterized in the operating frequency range, the material properties of the UV and epoxy glue are taken for W-band from [45]. The insertion loss is increased from the initial simulation model from 1.2 dB to 2.2 dB. The remaining difference of the insertion loss between the optimized simulation model and measurement is caused by the complex assembly of the filter, which consists of five brass parts, five LC filled Rexolite cavities and two double layer electrode substrates. The slight frequency shift is caused by manufacturing tolerances. A wideband response for an intermediate center frequency can be seen in Fig. 15. The resonance frequency of the coupling resonators changes according to the desired bandwidth and no spurious resonances can be observed in the Ka-band.

Compared to Fig. 7 and Fig. 8, a small frequency shift upwards can be seen. This might be the result of manufacturing inaccuracies resulting in slightly smaller cavities. The losses of the filter structure make a bandwidth analysis at the return loss level not practical. For this reason, the 3-dB bandwidth

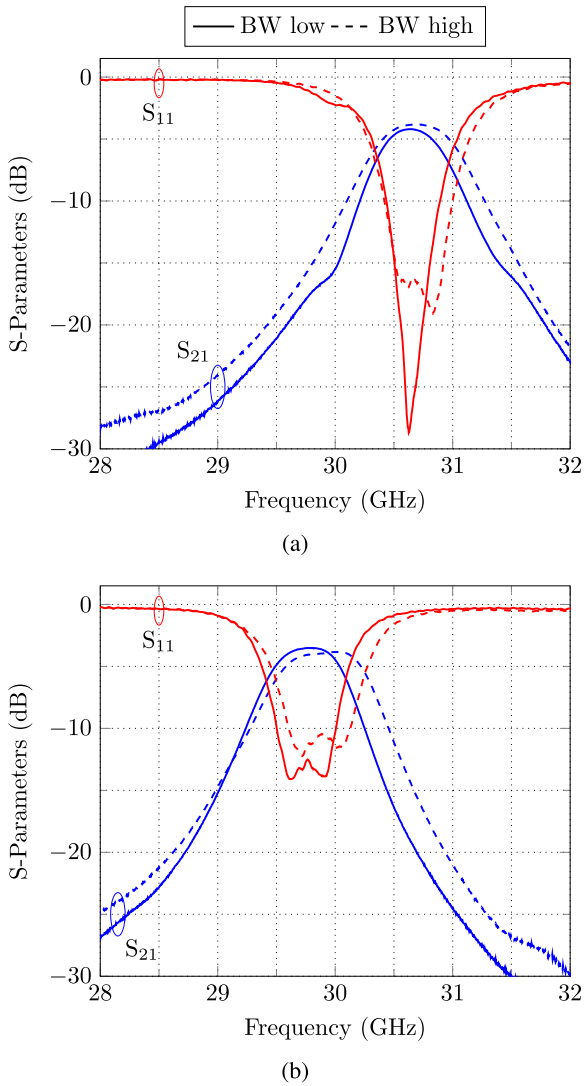

FIGURE 13. **Measured S-parameters for low and high bandwidth configuration for orthogonal (high center frequency) 13(a) and parallel (low center frequency) 13(b) LC orientation of the MRs resulting in a $f_0 \approx 30.7$ GHz and $f_0 \approx 29.8$ GHz, respectively. The 3-dB bandwidths are tuned from 654 MHz to 827 MHz and from 717 MHz to 871 MHz, respectively.**

is taken as a comparable value to analyze different tuning states. The 3-dB bandwidth is defined by the bandwidth where the maximum of S_{21} is decreased by 3 dB. To achieve different tuning states, the bias voltage is varied and, therefore, the permittivity of the LC changed. This results in different resonance frequencies and is used to adapt both the center frequency and the coupling. In Fig. 16, the 3-dB bandwidth of different measurement results are taken and plotted over their respective center frequency. The dotted area represents all center frequency/bandwidth combinations which are realizable, since the coupling strength can be adjusted continuously. It is noticeable that a higher 3-dB bandwidth can be realized compared to the simulations. This is related to the higher losses, which cause a widening of the passband. A wide range of different bandwidth/center frequency combinations can be

TABLE 1. Summary of State-of-The-Art Liquid Crystal Bandpass Filters

Work	Topology	f_c tuning	BW tuning	f(GHz)	FBW	τ_{f_c}	τ_{BW}	IL(dB)
[46]	Microstrip	yes	no	50 GHz	18 %	10.3 %	/	3.8
[46]	Microstrip	yes	no	85 GHz	16.5 %	10.4 %	/	7.6
[47]	Microstrip	yes	no	33 GHz	10 %	5.7 %	/	4.5
[48]	Microstrip	yes	no	40 GHz	19.8 %	3.9 %	/	3.9
[49]	SIW	yes	no	30 GHz	11.4 %	2.3 %	/	2 - 4
[19]	HMCSIW	yes	no	16.5 GHz	3.9 %	3.8 %	/	3.4
[20]	NRD	yes	no	60 GHz	1 %	2.9 %	/	4.2 - 6.2
[18]	Waveguide	yes	no	20 GHz	1 %	2.3 %	/	5.0 -7.0
This	Waveguide	yes	yes	30 GHz	1 %	3 %	24 %	3.5 - 4.2

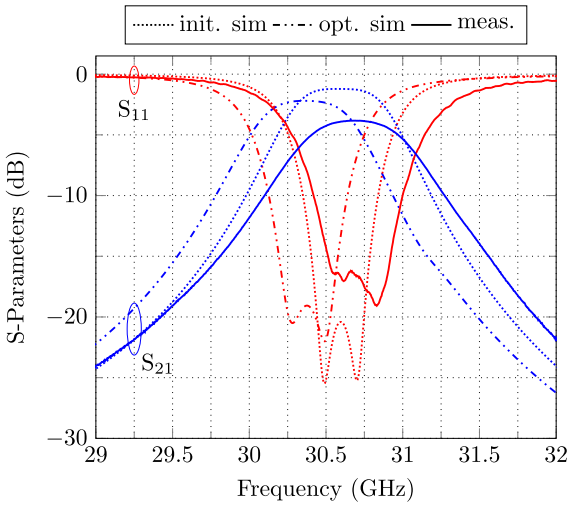

FIGURE 14. S-Parameters of different simulation models in comparison with a measured response. The initial simulation model includes the losses of the LC, Rexolite and conductivity losses of the brass casing. The optimized simulation model additionally includes the influence of the electrodes and the UV and epoxy adhesives of the Rexolite cavities. The frequency shift is caused by manufacturing tolerances.

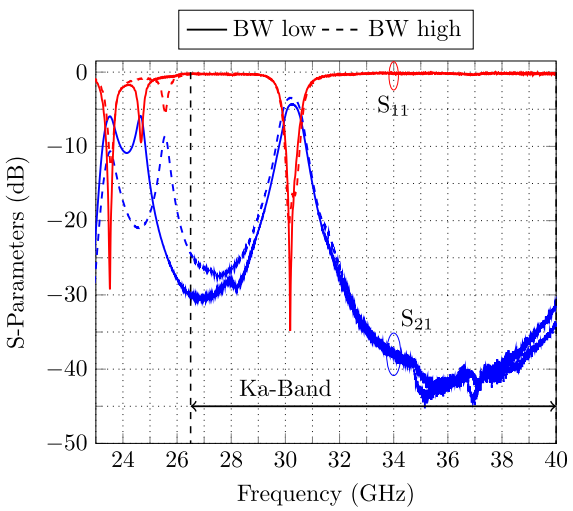

FIGURE 15. Measured wideband S-parameter response for different tuning states at $f_0 = 30.25$ GHz. The resonance frequency of the CR changes according to the bandwidth.

seen, which highlights the reconfigurability of the presented microwave filter. A minimum bandwidth variation between

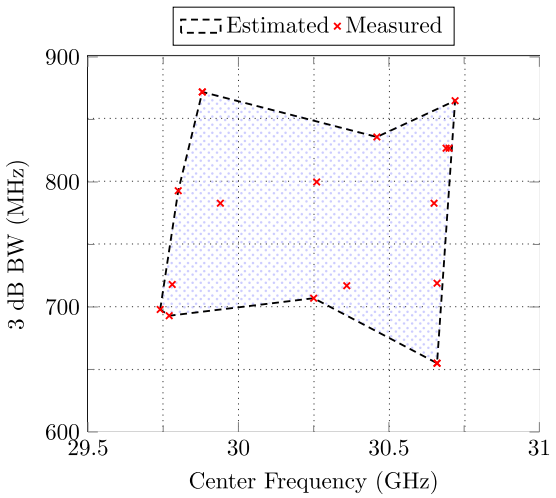

FIGURE 16. Range of measured 3-dB bandwidths for different center frequencies. Dotted area represents realizable configurations.

720 MHz to 840 MHz can be achieved for a center frequency range from 29.8 GHz to 30.7 GHz. In Table 1 a summary of state-of-the-art liquid crystal bandpass filters in different topologies is given. Only the filter presented in this work is tunable in both center frequency and bandwidth. For filter with larger FBW, e.g. [46] and [47], larger tunability of the center frequency can be obtained. Although this work consists of a filter with tunable coupling resonators, the insertion loss is lower as other narrowband filter e.g. [20] and [18].

VII. CONCLUSION

In this paper a fully reconfigurable bandpass filter in Ka-band is presented. To the best of the authors knowledge, this is the first time that a center frequency and bandwidth tunable LC bandpass filter is presented. First, the general properties of LCs are highlighted and the theory for the reconfigurable filter is explained. Afterwards, the design process for a two pole bandpass filter with tunable main and coupling resonators are shown. In addition, a novel electrode design is presented that allows electrical tuning of the LC molecules in a closed metallic waveguide. Finally, the simulated filter manufactured and the measurement results are analyzed. The measurement results show a high bandwidth and center frequency variation, where the center frequency can be varied between 29.8 GHz

to 30.7 GHz, while the 3-dB bandwidth can be changed between 660 MHz and 870 MHz. This results in a maxiumum bandwidth variation of over 24%.

REFERENCES

[1] Y. Huo, X. Dong, and W. Xu, "5G cellular user equipment: From theory to practical hardware design," *IEEE Access*, vol. 5, pp. 13992–14010, Jul. 2017, doi: 10.1109/ACCESS.2017.2727550.

[2] T. Weiss and F. Jondral, "Spectrum pooling: An innovative strategy for the enhancement of spectrum efficiency," *IEEE Commun. Mag.*, vol. 42, no. 3, pp. S 8–14, Mar. 2004.

[3] W. Cheng, H. Zhang, L. Liang, H. Jing, and Z. Li, "Orbital-angular-momentum embedded massive MIMO: Achieving multiplicative spectrum-efficiency for mmWave communications," *IEEE Access*, vol. 6, pp. 2732–2745, Dec. 2018, doi: 10.1109/ACCESS.2017.2785125.

[4] S. Maleki *et al.*, "Cognitive spectrum utilization in Ka band multibeam satellite communications," *IEEE Commun. Mag.*, vol. 53, no. 3, pp. 24–29, Mar. 2015.

[5] G. Raleigh and V. Jones, "Multivariate modulation and coding for wireless communication," *IEEE J. Sel. Areas Commun.*, vol. 17, no. 5, pp. 851–866, May 1999.

[6] M. Xiao *et al.*, "Millimeter wave communications for future mobile networks," *IEEE J. Sel. Areas Commun.*, vol. 35, no. 9, pp. 1909–1935, Sep. 2017.

[7] Z. Pi and F. Khan, "An introduction to millimeter-wave mobile broadband systems," *IEEE Commun. Mag.*, vol. 49, no. 6, pp. 101–107, Jun. 2011.

[8] F. Agnelli *et al.*, "Wireless multi-standard terminals: System analysis and design of a reconfigurable RF front-end," *IEEE Circuits Syst. Mag.*, vol. 6, no. 1, pp. 38–59, Jan.–Mar. 2006.

[9] S. Kanamaluru, "Tunable and reconfigurable filters [from the guest editor's desk]," *IEEE Microw. Mag.*, vol. 10, no. 6, pp. 8–12, Oct. 2009.

[10] G. Hattab and M. Ibnkahla, "Multiband spectrum access: Great promises for future cognitive radio networks," *Proc. IEEE*, vol. 102, no. 3, pp. 282–306, Mar. 2014.

[11] C.-K. Luo and J. F. Buckwalter, "A 0.25-to-2.25GHz, 27dBm IIP3, 16-path tunable bandpass filter," *IEEE Microw. Wireless Compon. Lett.*, vol. 24, no. 12, pp. 866–868, Dec. 2014.

[12] Y.-C. Hsiao, C. Meng, and S.-T. Yang, "5/60GHz 0.18μm CMOS dual-mode dual- conversion receiver using a tunable active filter for 5-GHz channel selection," *IEEE Microw. Wireless Compon. Lett.*, vol. 26, no. 11, pp. 951–953, Nov. 2016.

[13] M. S. Arif and D. Peroulis, "A 6 to 24GHz continuously tunable, microfabricated, high-Q cavity resonator with electrostatic MEMS actuation," in *IEEE/MTT-S Int. Microw. Symp. Dig.*, 2012, pp. 1–3.

[14] Z. Yang and D. Peroulis, "A 23-35 GHz mems tunable all-silicon cavity filter with stability characterization up to 140 million cycles," in *Proc. IEEE MTT-S Int. Microw. Symp.*, 2014, pp. 1–4.

[15] A. Tombak, F. Ayguavives, J.-P. Maria, G. Stauf, A. Kingon, and A. Mortazawi, "Tunable RF filters using thin film barium strontium titanate based capacitors," in *IEEE MTT-S Int. Microw. Symp. Dig. (Cat. No.01CH37157)*, 2001, vol. 3, pp. 1453–1456.

[16] C. Schuster *et al.*, "Performance analysis of reconfigurable bandpass filters with continuously tunable center frequency and bandwidth," *IEEE Trans. Microw. Theory Techn.*, vol. 65, no. 11, pp. 4572–4583, Nov. 2017.

[17] C. Schuster *et al.*, "Fully reconfigurable bandpass with continuously tunable center frequency and bandwidth featuring a constant filter characteristic," in *Proc. German Microw. Conf.*, 2020, pp. 236–239.

[18] T. Franke, A. Gaebler, A. E. Prasetiadi, and R. Jakoby, "Tunable Ka-band waveguide resonators and a small band band-pass filter based on liquid crystals," in *Proc. 44th Eur. Microw. Conf.*, 2014, pp. 339–342.

[19] D. Jiang, Y. Liu, X. Li, G. Wang, and Z. Zheng, "Tunable microwave bandpass filters with complementary split ring resonator and liquid crystal materials," *IEEE Access*, vol. 7, pp. 126265–126272, Jun. 2019, doi: 10.1109/ACCESS.2019.2924194.

[20] E. Polat *et al.*, "Tunable liquid crystal filter in nonradiative dielectric waveguide technology at 60GHz," *IEEE Microw. Wireless Compon. Lett.*, vol. 29, no. 1, pp. 44–46, Jan. 2019.

[21] F. Huang, S. Fouladi, M. Nasresfahani, and R. R. Mansour, "Three dimensional tunable filters with absolute constant bandwidth and method," U.S. Patent US20 160 049 710A1, Aug. 2018.

[22] U. Rosenberg *et al.*, "Novel remote controlled dual mode filter providing flexible re-allocation of center frequency and bandwidth," in *Proc. IEEE MTT-S Int. Microw. Symp.*, 2016, pp. 1–3.

[23] C. Weickhmann, "Liquid crystals towards terahertz: Characterisation and tunable waveguide phase shifters for millimetre-wave and terahertz beamsteering antennas," Ph.D. dissertation, Dept. Elect. Eng. Inf. Technol., Technische Universität Darmstadt, May 2017.

[24] E. Polat *et al.*, "Characterization of liquid crystals using a temperature-controlled 60GHz resonator," in *Proc. IEEE MTT-S Int. Microw. Workshop Ser. Adv. Mater. Process. RF THz Appl.*, 2019, pp. 19–21.

[25] F. Goelden, S. Mueller, P. Scheele, M. Wittek, and R. Jakoby, "IP3 measurements of liquid crystals at microwave frequencies," in *Proc. Eur. Microw. Conf.*, Sep. 2006, pp. 971–974.

[26] T. Kaesser, C. Fritzsch, and M. Franz, "Tunable RF filters based on liquid crystal for space applications," *Crystals*, vol. 10, no. 6, May 2020, Art. no. 455, doi: 10.3390/cryst10060455.

[27] M. Schallner, B. Friedrichs, and F. Ortwein, "Verification of new technologies as main task of the communication payload of the Heinrich-Hertz mission," *CEAS Space J.*, vol. 2, no. 1, pp. 67–73, Dec. 2011.

[28] W. Xu *et al.*, "Tunable bandstop HMSIW filter with flexible center frequency and bandwidth using liquid crystal," *IEEE Access*, vol. 7, pp. 161308–161317, Nov. 2019, doi: 10.1109/ACCESS.2019.2951543.

[29] E. Polat, R. Reese, H. Tesmer, M. Nickel, R. Jakoby, and H. Maune, "Fully dielectric phased array for beamsteering using liquid crystal technology at W-band," in *Proc. 14th Eur. Conf. Antennas Propag.*, 2020, pp. 1–5.

[30] R. Reese, M. Jost, E. Polat, M. Nickel, R. Jakoby, and H. Maune, "A dielectric waveguide switch based on tunable multimode interference at W-band," in *Proc. IEEE/MTT-S Int. Microw. Symp.*, 2018, pp. 179–182.

[31] E. Polat *et al.*, "Liquid crystal phase shifter based on nonradiative dielectric waveguide topology at W-band," in *Proc. IEEE MTT-S Int. Microw. Symp.*, 2019, pp. 184–187.

[32] M. Nickel *et al.*, "Liquid crystal based tunable reflection-type power divider," in *Proc. 48th Eur. Microw. Conf.*, 2018, pp. 45–48.

[33] E. Polat *et al.*, "Reconfigurable millimeter-wave components based on liquid crystal technology for smart applications," *Crystals*, vol. 10, no. 5, p. 346, Apr. 2020, doi: 10.3390/cryst10050346.

[34] P. Ferrari, R. Jakoby, O. H. Karabey, G. Rehder, and H. Maune, *Reconfigurable Circuits and Technologies for Smart Millimeter-Wave Systems (EuMA High Frequency Technologies Series)*. New York, NY, USA: Cambridge Univ. Press, 2021. [Online]. Available: https://www.cambridge.org/us/academic/subjects/engineering/rf-and-microwave-engineering/reconfigurable-circuits-and-technologies-smart-millimeter-wave-systems?format=HB

[35] R. Jakoby, A. Gaebler, and C. Weickhmann, "Microwave liquid crystal enabling technology for electronically steerable antennas in SATCOM and 5G millimeter-wave systems," *Crystals*, vol. 10, no. 6, p. 514, Apr. 2020, doi: 10.3390/cryst10060514.

[36] M. Wittek, C. Fritzsch, and D. Schroth, "Employing liquid crystal-based smart antennas for satellite and terrestrial communication," *Inf. Display*, vol. 37, no. 1, pp. 17–22, Jan. 2021.

[37] C. Arnod, J. Parlebas, and T. Zwick, "Center frequency and bandwidth tunable waveguide bandpass filter with transmission zeros," in *Proc. Eur. Microw. Conf.*, 2015, pp. pp. 369–372.

[38] R. J. Cameron, C. M. Kudsia, and R. R. Mansour, *Microwave Filters for Communication Systems*, 2nd ed. Hoboken, NJ, USA: Wiley, Apr. 2018. [Online]. Available: https://www.wiley.com/en-cx/Microwave+Filters+for+Communication+Systems%3A+Fundamentals%2C+Design%2C+and+Applications%2C+2nd+Edition-p-9781118274347

[39] C. Arnold, J. Parlebas, and T. Zwick, "Reconfigurable waveguide filter with variable bandwidth and center frequency," *IEEE Trans. Microw. Theory Techn.*, vol. 62, no. 8, pp. 1663–1670, Aug. 2014.

[40] F. Kamrath, D. Miek, P. Boe, and M. Höft, "Fully reconfigurable bandpass filter with coupling resonators and arbitrary transmission zero position," in *Proc. IEEE Asia-Pacific Microw. Conf.*, 2020, pp. 938–940.

[41] A. G. Lamperez, T. K. Sarkar, and M. S. Palma, "Filter model generation from scattering parameters using the cauchy method," in *Proc. 32nd Eur. Microw. Conf.*, 2002, pp. 1–4.

[42] J.-S. Hong and M. J. Lancaster, *Microstrip Filters for RF/Microwave Applications*. Hoboken, NJ, USA: Wiley, Mar. 2004.

[43] R. Reese *et al.*, "A millimeter-wave beam-steering lens antenna with reconfigurable aperture using liquid crystal," *IEEE Trans. Antennas Propag.*, vol. 67, no. 8, pp. 5313–5324, Aug. 2019.
[44] C. Weickhmann, N. Nathrath, R. Gehring, A. Gaebler, M. Jost, and R. Jakoby, "A light-weight tunable liquid crystal phase shifter for an efficient phased array antenna," in *Proc. Eur. Microw. Conf.*, 2013, pp. 428–431.
[45] H. Tesmer, R. Razzouk, E. Polat, D. Wang, R. Jakoby, and H. Maune, "Temperature characterization of liquid crystal dielectric image line phase shifter for millimeter-wave applications," *Crystals*, vol. 11, no. 1, p. 63, 2021, doi: 10.3390/cryst11010063.
[46] E. C. Economou *et al.*, "Electrically tunable open-stub bandpass filters based on nematic liquid crystals," *Phys. Rev. Appl.*, vol. 8, Dec 2017, Art. no. 064012, doi: 10.1103/PhysRevApplied.8.064012.
[47] M. Yazdanpanahi and D. Mirshekar-Syahkal, "Millimeter-wave liquid-crystal-based tunable bandpass filter," in *Proc. IEEE Radio Wireless Symp.*, 2012, pp. 139–142.
[48] Y. Liu, L. Zeng, S. Zhou, L. Li, and S. McGrath, "A wideband millimeter-wave tunable filter based on periodic square spiral structure and liquid crystal material," in *Proc. 31st Ir. Signals Syst. Conf.*, 2020, pp. 1–4.
[49] A. E. Prasetiadi *et al.*, "Liquid-crystal-based amplitude tuner and tunable SIW filter fabricated in LTCC technology," *Int. J. Microw. Wireless Technol.*, vol. 10, no. 5–6, pp. 674–681, 2018.

FYNN KAMRATH received the B.Sc. and M.Sc. degrees in 2017 and 2019, respectively, in electrical engineering and information technology from the University of Kiel, Kiel, Germany, where he is currently working toward the Dr.-Ing. degree with the Chair of Microwave Engineering, Institute of Electrical Engineering and Information Technology. His current research interests include the design, realization, and optimization of center frequency and bandwidth tunable microwave filters.

ERSIN POLAT was born in Alzenau, Germany, in 1991. He received the B.Sc. and M.Sc. degrees in 2014 and 2017, respectively, in electrical engineering and information theory from Technische Universität Darmstadt, Darmstadt, Germany, where he is currently working toward the Ph.D. degree with Microwave Engineering Group. His current research interests include tunable microwave filters based on liquid crystal technology and material characterization.

STIPO MATIC was born in Wiesbaden, Germany, in 1991. He received the B.Sc. and M.Sc. degrees in 2017 and 2020, respectively, from Technische Universität Darmstadt, Darmstadt, Germany, where he is currently working toward the Ph.D. degree with the Institute for Microwave Engineering and Photonics. His current research interests include the design and integration of reconfigurable components based on the ferroelectric material barium strontium titanate.

CHRISTIAN SCHUSTER was born in Wiesbaden, Germany, in 1988. He received the B.Sc. and M.Sc. degrees in 2012 and 2015, respectively, from Technische Universität Darmstadt, Darmstadt, Germany, where he is currently working toward the Ph.D. degree with Microwave Engineering Group. His research interests include tunable microwave filters and reconfigurable RF transceiver systems.

DANIEL MIEK (Student Member, IEEE) received the B.Sc. and M.Sc. degrees in 2015 and 2017, respectively, in electrical engineering and information technology from the University of Kiel, Kiel, Germany, where he is currently working toward the Dr.-Ing. degree with the Chair of Microwave Engineering, Institute of Electrical Engineering and Information Technology. His current research interests include the design, realization, and optimization of microwave filters and also parameter extraction and computer aided tuning.

HENNING TESMER was born in Kassel, Germany, in 1992. He received the B.Sc. and M.Sc. degrees in 2015 and 2018, respectively, from Technische Universität Darmstadt, Darmstadt, Germany, where he is currently working toward the Ph.D. degree with the Institute of Microwave Engineering and Photonics. His current research interests include liquid crystal-based tunable dielectric waveguides and components for millimeter-wave applications.

PATRICK BOE (Student Member, IEEE) received the B.Sc. and M.Sc. degrees in electrical engineering, information technology, and business management from Kiel University, Kiel, Germany, in 2017 and 2019, respectively. He is currently working toward the Dr.-Ing. degree as a Member of the Chair of Microwave Engineering with the Institute of Electrical Engineering and Information Technology. His current research interests include the design, realization and optimization of dielectric resonator filters and also dielectric multi-mode filters.

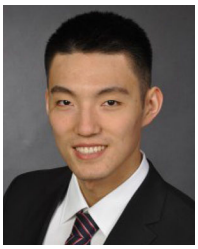

DONGWEI WANG was born in Taiyuan, Shanxi, China, in 1991. He received the B.Eng. degree from Zhejiang University, Hangzhou, Zhejiang, China, and the M.Sc. degree from Karlsruher Institut für Technologie, Karlsruhe, Germany. He is currently working toward the Ph.D. degree with the Institute of Microwave Engineering and Photonics, Technische Universität Darmstadt, Darmstadt, Germany. His current research focuses on liquid crystal-based tunable planar devices with slow-wave effect.

ROLF JAKOBY (Member, IEEE) was born in Kinheim, Germany, in 1958. He received the Dipl.-Ing. and Dr.-Ing. degrees in electrical engineering from the University of Siegen, Germany, in 1985 and 1990, respectively. In 1991, he joined the Research Center of Deutsche Telekom, Darmstadt, Germany. Since 1997, he has been a Full Professor with Technische Universität Darmstadt, Germany. He is a Co-Founder of ALCAN Systems GmbH. He has authored more than 320 publications. He holds more than 20 patents. His research interests include chipless RFID sensor tags, biomedical sensors and applicators, tunable passive microwave/millimeter wave devices, and beam-steering antennas, using primarily ferroelectric and liquidcrystal technologies. He is also a Member of VDE/ITG and IEEE/MTT/AP Societies. He was the recipient of the Award from CCI Siegen for his excellent Ph.D. in 1992 and the ITG-Prize for an excellent publication in the IEEE Transactions on Antennas and Propagation in 1997. His group was the recipient of the 23 awards and Prizes for best articles and doctoral dissertations. He is also the Editor-in-Chief of the FREQUENZ and DeGruyter. He was the Chairman of the EuMC in 2007 and the GeMiC in 2011, and the Treasurer of the EuMW in 2013 and 2017, respectively.

HOLGER MAUNE (Senior Member, IEEE) was born in Cologne, Germany, in 1981. He received the Dipl.-Ing., Dr.-Ing., and Venia Legend degrees in communications engineering from the Technische Universitaet Darmstadt, Darmstadt, Germany, in 2006, 2011, and 2020, respectively. Since 2021, he has been a Full Professor of electrical engineering and holds the Chair of Microwave and Communication Engineering with the University of Magdeburg, Germany. His research focuses on reconfigurable smart radio frequency (RF) systems based on electronically tunable microwave components, such as phase shifters, adaptive matching networks, tunable filters, duplexer, and multiband antennas. Their integration into system components such as adaptively matched power amplifiers, reconfigurable RF frontends or fully integrated electronically beam-steering transceiver antenna arrays is in the focus of the work.

MICHAEL HÖFT (Senior Member, IEEE) received the Dipl.-Ing. degree in electrical engineering and the Dr.-Ing. degree from the Hamburg University of Technology, Hamburg, Germany, in 1997 and 2002, respectively. From 2002 to 2013, he was with Communications Laboratory, European Technology Center, Panasonic Industrial Devices Europe GmbH, Lüneburg, Germany. He was a Research Engineer and the Team Leader, where he was involved in the research and development of microwave circuitry and components, particularly filters for cellular radio communications. From 2010 to 2013, he was also the Group Leader of the research and development of sensor and network devices. Since 2013, he has been a Full Professor with the Faculty of Engineering, Kiel University, Kiel, Germany, where he is currently the Head of the Chair of Microwave Engineering, Institute of Electrical Engineering and Information Technology. His research interests include active and passive microwave components, sub-millimeter-wave quasi-optical techniques and circuitry, microwave and field measurement techniques, microwave filters, microwave sensors, and magnetic field sensors. He is a Member of the European Microwave Association, the Association of German Engineers, and the German Institute of Electrical Engineers.